Journal of Computational Electronics X:YYY-ZZZ,200?
©2006 Springer Science Business Media, Inc. *Manufactured in The Netherlands*

# Discontinuous Galerkin Solver for Boltzmann-Poisson Transients

Yingda Cheng, Irene M. Gamba
*Department of Mathematics and ICES, The University of Texas at Austin, USA*
ycheng@math.utexas.edu, gamba@math.utexas.edu

Armando Majorana
*Dipartimento di Matematica e Informatica, Università di Catania, Catania, Italy*
majorana@dmi.unict.it

Chi-Wang Shu
*Division of Applied Mathematics, Brown University, Providence, RI 02912, USA*
shu@dam.brown.edu

**Abstract.** We present results of a discontinuous Galerkin scheme applied to deterministic computations of the transients for the Boltzmann-Poisson system describing electron transport in semiconductor devices. The collisional term models optical-phonon interactions which become dominant under strong energetic conditions corresponding to nano-scale active regions under applied bias. The proposed numerical technique is a finite element method using discontinuous piecewise polynomials as basis functions on unstructured meshes. It is applied to simulate hot electron transport in bulk silicon, in a silicon $n^+$-$n$-$n^+$ diode and in a double gated 12nm MOSFET. Additionally, the obtained results are compared to those of a high order WENO scheme simulation.

**Keywords:** Deterministic numerical methods, Discontinuous Galerkin schemes, Boltzmann Poisson systems, Statistical hot electron transport, Semiconductor nano scale devices.

## Introduction

In modern highly integrated devices, a consistent description of the dynamics of carriers is essential for a deeper understanding of the observed transport properties. The semi-classical Boltzmann-Poisson system is used and given by, for $\mathbf{E} = -\nabla_{\mathbf{x}} V$,

$$\frac{\partial f}{\partial t} + \frac{1}{\hbar}\nabla_{\mathbf{k}}\varepsilon \cdot \nabla_{\mathbf{x}} f - \frac{q}{\hbar}\mathbf{E} \cdot \nabla_{\mathbf{k}} f = Q(f), \qquad (1)$$

$$\mathrm{div}_{\mathbf{x}}(\epsilon_r(\mathbf{x})\nabla_{\mathbf{x}} V) = \frac{q}{\epsilon_0}\left[\rho(t,\mathbf{x}) - N_D(\mathbf{x})\right],$$

which provides a general theoretical framework for modeling electron transport. Time-dependent solutions of the Boltzmann-Poisson system contain all the information on the evolution of the carrier distribution. In Eq. (1), $f$ represents the electron probability density function (*pdf*) in phase space $\mathbf{k}$ at the physical location $\mathbf{x}$ and time $t$. $\mathbf{E}$ is the electric field and $\varepsilon$ is the energy-band function. Physical constants $\hbar$ and $q$ are the Planck constant divided by $2\pi$ and the positive electric charge, respectively. The parameter $\epsilon_0$ is the dielectric constant in a vacuum, $\epsilon_r(\mathbf{x})$ labels the relative dielectric function depending on the material, $\rho(t,\mathbf{x})$ is the electron density, and $N_D(\mathbf{x})$ is the doping. The collision operator $Q(f)$ describes electron-phonon interactions where most important ones in Si are due to scattering with lattice vibrations of the crystal, which are modeled by acoustic and optical non-polar modes with a single frequency $\omega_p$, i.e.

$$Q(f)(t,\mathbf{x},\mathbf{k}) = \int_{\mathbb{R}^3} \left[S(\mathbf{k}',\mathbf{k})f(t,\mathbf{x},\mathbf{k}') - S(\mathbf{k},\mathbf{k}')f(t,\mathbf{x},\mathbf{k})\right]\, d\mathbf{k}',$$

where $S(\mathbf{k}, \mathbf{k}')$ is defined by

$$\begin{aligned} S(\mathbf{k}, \mathbf{k}') &= K_0(\mathbf{k}, \mathbf{k}')\, \delta(\varepsilon(\mathbf{k}') - \varepsilon(\mathbf{k})) + K(\mathbf{k}, \mathbf{k}') \\ &\quad \times [(\mathsf{n}_q + 1)\, \delta(\varepsilon(\mathbf{k}') - \varepsilon(\mathbf{k}) + \hbar\omega_p) \\ &\quad + \mathsf{n}_q\, \delta(\varepsilon(\mathbf{k}') - \varepsilon(\mathbf{k}) - \hbar\omega_p)] \ . \end{aligned}$$

The phonon occupation factor is

$$\mathsf{n}_q = \left[ \exp\left( \frac{\hbar\omega_p}{k_B T_L} \right) - 1 \right]^{-1}$$

where $k_B$ is the Boltzmann constant and $T_L = 300°K$ is the constant lattice temperature. The symbol $\delta$ indicates the usual Dirac distribution.

## 1. Numerical method

Very recently, deterministic solvers to the Boltzmann-Poisson system (1) for two-dimensional devices were proposed [1–3, 7]. These methods provide accurate results which, in general, agree well with those obtained from Monte Carlo (DSMC) simulations, often at a fractional computational time. Moreover, they can resolve transient details for the *pdf*, which are difficult to compute with DSMC simulators. The methods proposed in [2, 3] used weighted essentially non-oscillatory (WENO) finite difference schemes to solve the Boltzmann-Poisson system. The advantage of the WENO scheme is that it is relatively simple to code and very stable even on coarse meshes for solutions containing sharp gradient regions. A disadvantage of the WENO finite difference method is that it requires smooth meshes to achieve high order accuracy, hence it is not very flexible for adaptive meshes. We report in this manuscript a discontinuous Galerkin (DG) method for solving the Boltzmann-Poisson system as developed in [5]. The DG method is a finite element method using discontinuous piecewise polynomial basis functions and relies on an adequate choice of numerical fluxes, which handle effectively the interactions across element boundaries. See for example the review paper [6] and references therein. Recent development of the locally discontinuous Galerkin methodology allows us to adopt a unified discretization strategy to handle all spatial derivatives in semiconductor device models including the Boltzmann-Poisson system [5, 8, 9], with an $L^2$ stable and locally conservative scheme having the potential for full *h-p* adaptivity.

## 2. Transformed equations and computational results

The transport equation (1) is written in band energy-spherical coordinates that can handle the singular energy masses in the scattering terms [10]. In fact, we perform a coordinate transformation for $\mathbf{k}$ according to

$$\begin{aligned} \mathbf{k} &= \frac{\sqrt{2m^* k_B T_L}}{\hbar} \sqrt{w(1 + k_B T_L \alpha w)} \\ &\quad \left( \mu, \sqrt{1-\mu^2}\cos\varphi, \sqrt{1-\mu^2}\sin\varphi \right), \end{aligned}$$

where the new independent variables are the dimensionless band energy $w$, the cosine of the polar angle $\mu$, and the azimuthal angle $\varphi$. The physical parameter $\alpha$ is related to the crystal conduction band. The new unknown charge distribution is

$$\Phi(t, x, y, z, w, \mu, \phi) = s(w) \tilde{f}(t, x, y, z, w, \mu, \phi) \ ,$$

where $s(w) = \sqrt{w(1 + \alpha_\kappa w)}(1 + 2\alpha_\kappa w)$ is related to the Jacobian of the coordinate transformation and the density of the states; and $\tilde{f}$ denotes $f$ in the new variables. The corresponding transformed dimensionless Boltzmann equation remains in conservative form [2]. The corresponding free streaming operator depends on the electric field $\mathbf{E}$. In particular, the numerical fluxes for the DG approximation should be taken carefully in an upwind fashion. For other details and physical constants we refer to [2–4] and the forthcoming publication [5].

## 3. Numerical results

For a 12 nm double gate MOSFET device (Fig. 1), Fig. 2 shows the hydrodynamic moments. In particular we stress the capability of DG solves to capture expected strong energy effects near the gates.

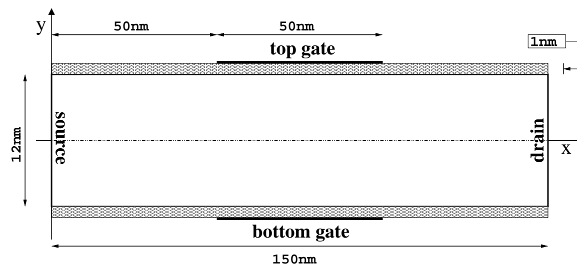


*Figure* 1: Double gate MOSFET

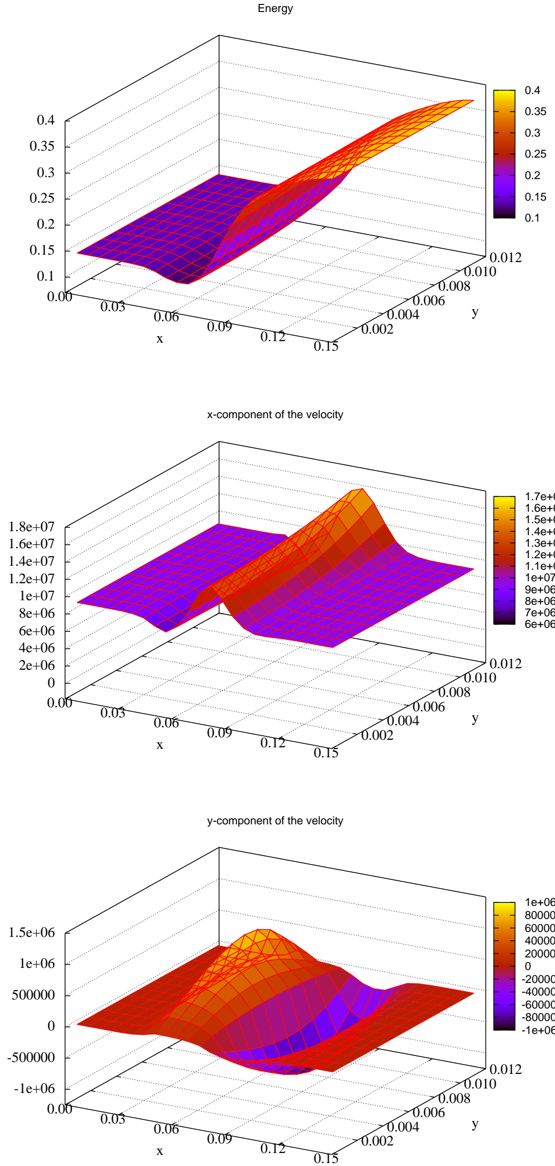


*Figure* 2: Symmetric half mirror simulation at 2 ps (stationary regime). Top: Kinetic energy (eV) Middle: $x$-component of the mean velocity (cm/s); Bottom: $y$-component of the mean velocity (cm/s).

For the one dimensional silicon $n^+ - n - n^+$ 50nm channel diode, where the doping $N_D = 5 \times 10^{18}$ cm$^{-3}$ in the n$^+$ and $N_D = 1 \times 10^{15}$ $cm^{-3}$ in the n region. We use a non-uniform grid with $64 \times 60 \times 20$ cells in the $(x, w, \mu)$ domain. The applied voltage is $1eV$ in all simulations. The simulation results at steady states for $t = 2ps$ are shown. Figure 3 shows a computed stationary $pdf$ at the location $x = 0.125$ micron in the middle of the 50 nm channel, both in the scaled band energy-spherical and cartesian coordinates in velocity space.

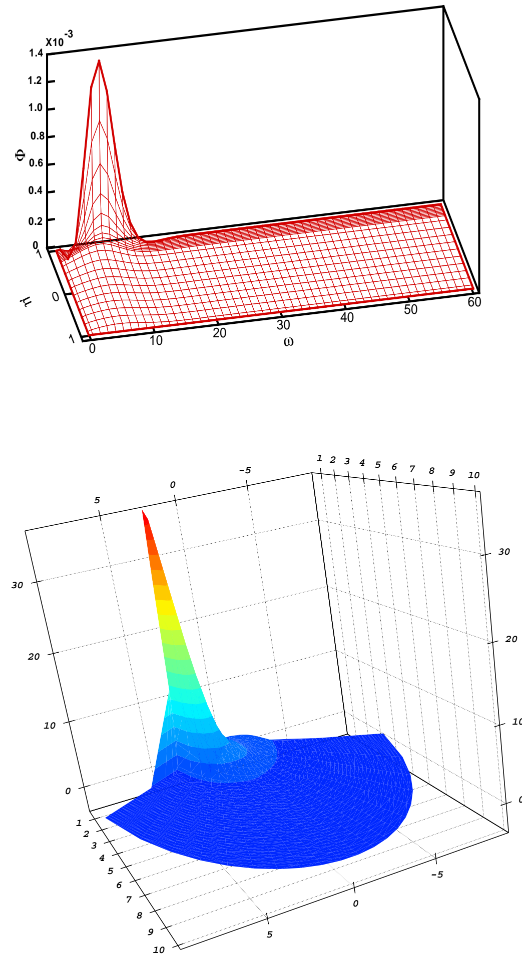


*Figure* 3: $pdf$ in the stationary regime at the middle of the 50nm channel device. Top: the scaled pdf $\Phi$ in the $(w,\mu)$ coordinates; bottom: the pdf $f$ in $(k_1, \sqrt{k_2^2 + k_3^2})$ coordinates.

A comparison between WENO vs DSMC, in Fig. 4, is performed for a 50nm channel. Figure 5 shows DG results using different meshes.

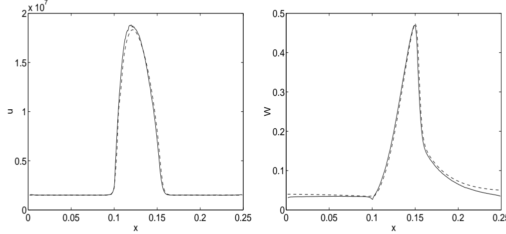


*Figure* 4: Comparisons for the 50 nm channel at $1eV$ Vbias time 2ps; full BP system by the DSMC method (solid line) and by the deterministic WENO solver (dashed line). **Left**: mean velocities in $cm/sec$; **right:** kinetic energies in $eV$.

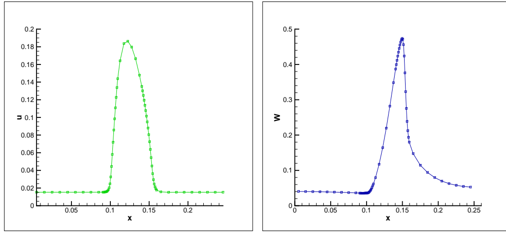


*Figure* 5: Comparisons for the 50 nm channel at $1V$ Vbias time 2ps. DG scheme with non-uniform mesh. **Left**: mean velocities in $cm/sec$; **right:** kinetic energies in $eV$.

Finally, a comparison between DG and WENO for a 400nm channel is shown in Fig. 6. We note the superiority of the DG scheme to compute the numerical moment (Fig. 6, top left).

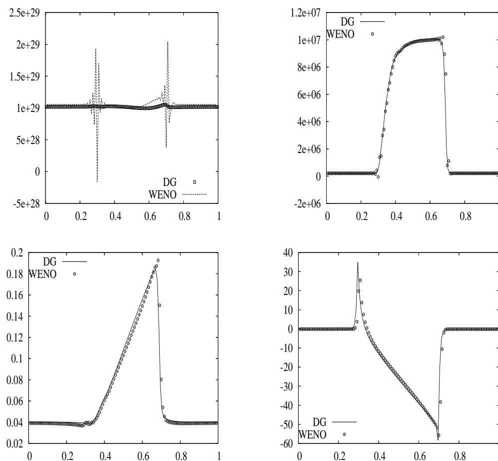


*Figure* 6: Comparisons for the 400 nm channel diode between WENO and DG solvers at $1V$ Vbias and $5ps$. **Top**: current (first moment), mean velocity. **Bottom**: kinetic energy, electric field.

The transient behavior for a simple bulk device with a constant electric field ($30KV/cm$) is shown in [4] Fig. 1-3, where the numerical DG and WENO vs DSMC solutions are compared.

## Acknowledgment

The first and fourth authors are supported in part by NSF grants DMS-0510345 and AST-0506734, and the second one by NSF under grant DMS-0507038. The third author acknowledges the nancial support by the EU Marie Curie RTN project COMSON - MRTN-CT-2005-019417 and Italian PRIN 2006. Support from ICES at UT Austin is also gratefully acknowledged.

## References

1. M.J. Caceres, J.A. Carrillo, I.M. Gamba, A. Majorana and C.-W. Shu, *Deterministic kinetic solvers for charged particle transport in semiconductor devices*, in Transport Phenomena and Kinetic Theory Applications to Gases, Semiconductors, Photons, and Biological Systems. C. Cercignani and E. Gabetta (Eds.), Birkhäuser (2006), pp. 151-171.
2. J.A. Carrillo, I.M. Gamba, A. Majorana and C.-W. Shu, *A direct solver for 2D non-stationary Boltzmann-Poisson systems for semiconductor devices: a MESFET simulation by WENO-Boltzmann schemes* , Journal of Computational Electronics, **2** (2003), pp. 375-380.
3. J.A. Carrillo, I.M. Gamba, A. Majorana and C.-W. Shu, *2D semiconductor device simulations by WENO-Boltzmann schemes: efficiency, boundary conditions and comparison to Monte Carlo methods*, Journal of Computational Physics, **214** (2006), pp. 55-80.
4. Y. Cheng, I.M. Gamba, A. Majorana and C.-W. Shu, *Discontinuous Galerkin Solver for the Semiconductor Boltzmann Equation*, SISPAD 07, T. Grasser and S. Selberherr, editors, Springer (2007) pp. 257-260.
5. Y. Cheng, I.M. Gamba, A. Majorana and C.-W. Shu, *Discontinuous Galerkin adaptive solver for Boltzmann Poisson systems in nano devices*, to appear.
6. B. Cockburn and C.-W. Shu, *Runge-Kutta discontinuous Galerkin methods for convection-dominated problems*, Journal of Scientific Computing, **16** (2001), pp. 173-261.
7. M. Galler, and A. Majorana, *Deterministic and stochastic simulation of electron transport in semiconductors*, to appear in Bulletin of the Institute of Mathematics, Academia Sinica (New Series), 6th MAFPD (Kyoto) special issue Vol. 2 (2007), No. 2, pp. 349-365.
8. I.M. Gamba and J. Proft, *Stable Discontinuous Galerkin Schemes for Linear Vlasov-Boltzmann Transport Equations*, ICES Report 07-25, submitted for publication (2007).
9. Y.-X. Liu and C.-W. Shu, *Local discontinuous Galerkin methods for moment models in device simulations: Performance assessment and two dimensional results*, Applied Numerical Mathematics, **57** (2007), pp. 629-645.
10. A. Majorana and R. Pidatella, *A finite difference scheme solving the Boltzmann Poisson system for semiconductor devices*, Journal of Computational Physics, **174** (2001), pp. 649-668.